

Picture change error correction in the radial distributions of canonical orbital densities and total electron density of radon atom: the effect of the size of nucleus and the basis set limit

Lukáš Bučinský · Stanislav Biskupič · Dylan Jayatilaka

Received: 4 March 2011 / Accepted: 7 March 2011 / Published online: 26 March 2011
© Springer-Verlag 2011

Abstract The 2nd order Douglas-Kroll-Hess (DKH2) and the Infinite Order Two Component (IOTC) radial distributions of electron density of canonical Hartree-Fock (HF) orbitals of radon atom are presented. Furthermore, the total electron density is revisited. The picture change error (PCE) correction is investigated by analytical means. The point charge model of nucleus and the Gaussian nucleus model are employed. The basis set is extrapolated by means of including tight s and also p Gaussians within the original triple zeta basis set. It is found that the DKH1 PCE corrected DKH2 total electron and s orbital contact densities are negative for the point charge model of nucleus if tight enough s Gaussians are included in the basis set. It is shown that this failure is caused due to the missing terms of the second order Douglas-Kroll transformation for the DKH2 electron density. PCE is found the most striking in the DKH2/IOTC electron density of s orbitals close to the nucleus. The radial distributions of the 2-component $p_{1/2}$ orbital densities are considerably affected by PCE at the nucleus as well. Furthermore, the PCE corrected DKH2/IOTC scalar p orbital densities have a non-zero value of electron density at nucleus and can be considered as an spin-orbit (SO) average of the $p_{1/2}$ and $p_{3/2}$ orbitals. The d and f orbitals are affected by PCE in the vicinity of the nucleus only little. The PCE corrected DKH2 and IOTC radial distributions of orbital densities are nodeless, which

is completely in agreement with the radial distribution of the analytic or numeric DCH orbital densities.

Keywords Picture change error · Picture change · Orbital density · Negative density · PCE correction · PCE

1 Introduction

The relativistic quantum chemistry has made a large progress in the last two decades [1–5]. The calculations at the Dirac-Coulomb Hamiltonian (DCH) level of theory became available [6–12]; in addition, the quasirelativistic approaches have moved from the lower order quasirelativistic Hamiltonians (DKH2, ZORA) [13–19] to the exact (or high order) diagonalization of the Dirac Hamiltonian and/or elimination of the small component [3, 20–32]. The X2C/IOTC approaches promise a quite straightforward implementation into the non-relativistic quantum chemistry packages and still have a favorable scaling in comparison with DCH calculations. Nevertheless, it is suggested that the Quasi 4-component (Q4C) DCH is of same demands as the 2-component quasirelativistic calculations, what has been denoted as “4-component and 2-component equally good” [31, 32].

Besides the improving scaling at the DCH level of theory, a further disadvantage of the quasirelativistic Hamiltonians is the picture change of the wavefunction, which gives rise to the picture change error (PCE) for property evaluation (expectation values, linear response property evaluation, etc.) [33–39]. While the PCE is by no means a problem for the obtained SCF energy [19], it might be an issue (and in most cases is an issue) in calculations of properties [33, 34, 36, 40, 41]. Especially, large PCE is to be found in electron density at nucleus

L. Bučinský (✉) · S. Biskupič
Institute of Physical Chemistry and Chemical Physics FCHPT,
Slovak University of Technology, Radlinskeho 9,
812 37 Bratislava, Slovakia
e-mail: lukas.bucinsky@stuba.sk

D. Jayatilaka
Department of Chemistry, University of Western Australia,
U35 Stirling Hwy, Crawley, WA 6009, Australia

(contact density) [35, 38, 39, 42, 43]. This is why properties which are closely related to the electron density in the vicinity of nucleus are sensitive to PCE [36, 40, 41].

To be mentioned is the work of Mastalerz et al. [35] who have presented the values of contact density of halogen atoms in the HX molecules (where X = F, Cl, Br, I, At) at different orders of DKH Hamiltonian and/or PCE correction using the Fermi nucleus model. Furthermore, in the work of Mastalerz et al. [35] has been presented the radial distribution of the hydrogen like Au^{78+} ion in the ground state (1s electron). Seino et al. [38] have considered the PCE correction of IOTC and DKH2 contact densities of several closed shell atoms. The contact density is the subject of the studies of Mastalerz et al. [42] and Knecht et al. [43] where the finite nucleus model is employed and the effects of electron correlation as well as basis set quality at nucleus is considered. In our previous study, we have considered the analytic correction and the extent of the PCE in the radial distributions of the total SCF electron density of radon atom at the DKH2 and IOTC levels of theory using the point charge model of nucleus [39]; nevertheless, the singularity issue of the relativistic contact density for the point charge nucleus model has not been studied in detail.

In the current study, the effect of the size of nucleus together with the basis set extrapolation in the radial distribution of electron density of radon atom is the goal. In addition, we are presenting the PCE and the relativistic effects in the radial distributions of canonical Hartree-Fock (HF) orbital densities of radon atom. Besides the *s* and *p* orbitals which are the most interesting in regard to PCE and relativistic effects, PCE and relativistic effects in the *d* and *f* orbitals are briefly discussed as well, i.e. chosen 1-component (1c) *s*, *p*, *d*, *f* orbital densities at NR, DKH2, IOTC level of Hamiltonian and 2-/4-component (2c/4c) $s_{1/2}$, $p_{1/2}$, $p_{3/2}$, $d_{3/2}$, $d_{5/2}$, $f_{5/2}$, $f_{7/2}$ DKH2, IOTC, DCH orbital densities are presented. The nodal behavior (PCE and relativistic effects) of the radial distributions of obtained orbital densities is presented as well.

2 Methods and computational details

The employed DKH2 Hamiltonian follows the original works of Hess and coworkers [15, 17–19, 25, 26]. The calculations at the IOTC level of theory were based on the approach of Barysz and Sadlej [21, 22, 24], the IOTC Y matrix was obtained by iterative means [22]. The picture change error correction of electron density has been described in our previous paper [39]. Furthermore, general PCE correction at the DKH and IOTC level has been in detail considered by Wolf and Reiher [33, 34] and Seino et al. [38], respectively.

The presented DKH2 and IOTC calculations and the PCE correction of electron density have been performed using a development version of the Tonto package [44]. Calculations at the DCH level of theory have been performed in the Grasp package [6] (numerical solution) and in the DIRAC10 package [45] (finite basis set approach). Furthermore, the DIRAC10 [45] package has been used to verify the NR, PCE contaminated as well as PCE corrected IOTC total electron and orbital densities and PCE contaminated DKH2 densities obtained in the Tonto package [44], as well as the implementation of the Gaussian nucleus model within a development version of the Tonto package [44].

The Gaussian model of nucleus [46] has been used to include the finite size nucleus effects. Besides, the uniformly charged sphere and the Fermi nucleus model [6, 46] have been employed as well, for comparison purposes [6]. The uncontracted triple zeta (UTZ) basis set ($30s26p17d11f$) has been predominantly used for the radon atom [47, 48]. Besides, a few benchmark calculations have been made using the uncontracted double zeta and quadruple zeta basis sets [47, 48], denoted as UDZ and UQZ, respectively. The UTZ basis set has been further expanded by up to 10 *s* and 5 *p* tight Gaussian functions (denoted as UTZ+NsMp, where N and M is the number of additional *s* and *p* tight Gaussians), to explore the basis set limits and basis set artifact of the total electron and orbital densities at and close to the point charge nucleus. The tight Gaussian functions were obtained by assuming an even tempered series for the tightest two Gaussians of the *s* and *p* blocks of the original UTZ basis set.

The radial distributions of the particular (*p*, *d*, *f*) orbital densities, which were calculated in the finite basis set approach, have been obtained by means of numerical averaging along the *x*-axis. In the case of the scalar (1-component) calculations the radial distributions of the orbital density along the *x*-axis of each degenerate $2l + 1$ orbital with the particular quantum numbers *n*, *l* have been summed up and divided by $2l + 1$. In the case of the 2-component (general complex) calculations the radial distributions of the $2j + 1$ degenerate orbitals with the particular quantum numbers *n*, *j* have been summed up and divided by $2j + 1$. The numerical integration of such averaged atomic orbital densities yields unambiguously an occupation number equal to 1, without any further scaling.

The obtained radial distributions at different levels of theory are labeled following the notation of Wolf and Reiher [33, 34], which was also employed in our previous paper on the total electron density of radon atom [39]:

- $\rho(\text{DCH})$ DCH electron density
- $\rho(\text{NR})$ NR electron density
- $\rho(\text{IOTC,IOTC})$ IOTC electron density which is corrected for PCE

- $\rho(IOTC,NR)$ IOTC electron density which is not PCE corrected (i.e. PCE contaminated electron density)
- $\rho(DKH2,DKH2)$ DKH2 electron density which is corrected for PCE up to the DKH2 order
- $\rho(DKH2,DKH1)$ DKH2 electron density which is corrected for PCE up to the DKH1 order
- $\rho(DKH2,DKH0)$ DKH2 electron density which is corrected for PCE up to the DKH0 order (only free particle Foldy-Wouthuysen transformation)
- $\rho(DKH2,NR)$ DKH2 electron density which is not PCE corrected (i.e. PCE contaminated electron density)

3 Results and discussions

3.1 Total electron density

3.1.1 Point charge nucleus

In Table 1 are presented the values of the contact densities of radon atom for the series of calculations using the UTZ+NsMp basis sets. The DCH, (IOTC,IOTC), (IOTC, NR), (DKH2,DKH2), (DKH2,DKH0) and (DKH2,NR) contact densities grow with the number of the tight Gaussians added to the original UTZ basis set, which is completely in agreement with the singular behavior of the relativistic contact density in the case of the point charge nucleus [3, 42]. On the other hand, the value of the (DKH2,DKH1) contact density is descending with the number of the tight s Gaussians added to the UTZ basis set and finally for basis sets which are larger than UTZ+4s the (DKH2,DKH1) contact density becomes negative. This feature has not been realized in our last study using the UTZ basis set [39]. What has been only found was a global maximum in the $\rho(DKH2,DKH1)$ density, which is not localized at the nucleus [39]. The global maximum is found shifted also in the radial distributions of the $\rho(DKH2,DKH1)$ densities calculated in the extended UTZ+Ns basis sets. An inspection of the contributions of the $X_{E,0}$, $X_{E,1}$ and $X_{E,2}$ terms [33, 39] (see Table 2) within the PCE corrected electron densities at the DKH2 level of theory shows that two of the eight $X_{E,1}$ terms which contain $A_p \delta(r) A_p$ and the P^2 factor explicitly are large and negative in value and cause that the $\rho(DKH2,DKH1)$ electron density in the vicinity of the point charge nucleus is negative if tight enough s Gaussians are included in the basis set. On the other hand, the $\{W_2, A_p \delta(r) A_p\}$ contributions [33, 39] of the $X_{E,2}$ term have a positive value, which is large enough in magnitude to damp the effect of the negative $X_{E,1}$ terms within the $\rho(DKH2,DKH2)$ density. Nevertheless, the final $\rho(DKH2, DKH2)$ contact densities are overestimated in comparison with $\rho(DCH)$ (see Table 1 and Fig. 1a) [38, 39]. In addition, this deviation is enlarged with the extension of the UTZ+Ns

basis set; in the case of the UTZ+10s basis set, the relative error between $\rho(DKH2,DKH2)$ and $\rho(DCH)$ is already 107%. The overestimated value of the $\rho(DKH2,DKH0)$ contact density (in regard of $\rho(DCH)$) is predominantly affected by the contribution of the $A_p \delta(r) A_p$ term within the $X_{E,0}$ term of PCE correction, see Table 2.

Nevertheless, the conclusions about the extent of the PCE remain the same as described previously for the UTZ basis set [39], i.e. the PCE leads to an overestimated electron density close to the nucleus at both the DKH2 as well as IOTC level of theory, see Table 1 and Fig. 1a. The $\rho(IOTC, IOTC)$ contact density copies the most the finite basis set value of $\rho(DCH)$ contact density for the series of UTZ+Ns calculations, see Table 1. The relative error between the $\rho(IOTC,IOTC)$ and $\rho(DCH)$ becomes smaller with the extension of the basis set. Furthermore, the $\rho(DCH)$ and $\rho(IOTC,IOTC)$ electron density distributions using the finite basis set approach and the UTZ+10s basis set are laying on top of each other, see Fig. 1a. The 2-component calculations improve slightly the agreement between the $\rho(IOTC,IOTC)$ and $\rho(DCH)$ densities at nucleus; see the results of the UTZ+10s calculations shown in Table 1.

For the UTZ+10s basis set, the basis set artifact becomes significant within the distance of $0.8 \times 10^{-7}\text{\AA}$ from the point charge nucleus, see Fig. 1a. In addition, the tests using the UDZ ($24s20p14d9f$) and UQZ ($34s31p21d14f1g$) basis sets have yielded quantitatively similar results of the $\rho(IOTC, IOTC)$ contact density (4.709808×10^6 , 4.744633×10^6 , respectively) as for the UTZ basis set (4.743935×10^6); thus, the basis set artifact can be most effectively treated only by adding tight enough s functions within the basis set, see Fig. 1d and Table 1. The extra p functions have an effect on the PCE corrected value of the DKH2 and IOTC contact densities only at the 2c level of theory, see Table 1.

It is noteworthy that the NR calculations using the basis sets with tight s Gaussians are numerically unstable and the calculations did not reach a proper convergence by means of DIIS (Direct Inversion in the Iterative Subspace) whether using the DIRAC10 or Tonto package. Although the NR contact densities do not show any unexpected behavior with the expansion of the UTZ+Ns basis set (see Table 1), they should be taken with care. The same holds for the NR calculations (contact densities) that use the finite (Gaussian) nucleus model, in Table 3.

3.1.2 Finite size nucleus

In the case of the Gaussian model of nucleus, it can be seen from Table 3 that with the growing number of tight s functions added to the UTZ basis set the contact densities have an oscillatory behavior.

Nevertheless, the PCE has qualitatively the same impact on the contact density and on the electron density close to

Table 1 The values of the (finite basis set approach) contact density (in $b\text{ohr}^{-3}$) of the radon atom for the point charge nucleus model, if not otherwise stated the quasirelativistic DKH2/IOTC values of electron densities are from the 1-component calculations

Basis set	DCH ^a	(IOTC, IOTC)	(DKH2, DKH2)	(DKH2, DKH1)	(DKH2, DKH0)	(IOTC, NR)	(DKH2, NR)	NR
UTZ [39]	4.819304E+06	4.743935E+06	5.648397E+06	2.599563E+06	8.848466E+06	1.629777E+07	1.533869E+07	4.547746E+05
UTZ+1s	6.431442E+06	6.351781E+06	8.061942E+06	2.693880E+06	1.257077E+07	2.423586E+07	2.233083E+07	4.562337E+05
UTZ+2s	8.643059E+06	8.557519E+06	1.161955E+07	2.528815E+06	1.782272E+07	3.599327E+07	3.227832E+07	4.570502E+05
UTZ+3s	1.154243E+07	1.144919E+07	1.662584E+07	1.868945E+06	2.494486E+07	5.283123E+07	4.588970E+07	4.574374E+05
UTZ+4s	1.550118E+07	1.539743E+07	2.384577E+07	5.394058E+05	3.477345E+07	7.737437E+07	6.48952E+07	4.576584E+05
UTZ+5s	2.070444E+07	2.058687E+07	3.390673E+07	-1.950791E+06	4.799514E+07	1.124931E+08	9.041215E+07	4.577595E+05
UTZ+6s	2.781263E+07	2.767619E+07	4.819545E+07	-5.946704E+06	6.602475E+07	1.634149E+08	1.254955E+08	4.578196E+05
UTZ+7s	3.7115585E+07	3.699461E+07	6.788475E+07	-1.242629E+07	9.0067556E+07	2.362066E+08	1.724699E+08	4.578458E+05
UTZ+8s	4.993204E+07	4.973689E+07	9.548757E+07	-2.204370E+07	1.225616E+08	3.415148E+08	2.361718E+08	4.578622E+05
UTZ+9s	6.671208E+07	6.647237E+07	1.331112E+08	-3.666724E+07	1.655215E+08	4.919454E+08	3.206313E+08	4.578689E+05
UTZ+10s	8.968274E+07	8.938202E+07	1.852692E+08	-5.749997E+07	2.231602E+08	7.093814E+08	4.342223E+08	4.578736E+05
UTZ+10s ^b	8.941575E+07	8.938345E+07	1.852709E+08	-5.749910E+07	2.232297E+08	7.090566E+08	4.340866E+08	4.578737E+05
UTZ+10s ^{1p}	8.970795E+07	8.939021E+07	1.852800E+08	-5.749613E+07	2.231754E+08	7.093813E+08	4.342223E+08	
UTZ+10s ^{5p}	8.992666E+07	8.962707E+07 ^b						

^a Dirac10 software package

^b 2-component DKH2/IOTC values

Table 2 The contributions to the DKH2 PCE corrected total electron density (in $bohr^{-3}$) of the radon atom

Nucleus model: r (Å); DKH terms	Gaussian	Point charge					
	0.0000E+00	0.0000E+00	1.0000E-09	1.0000E-08	1.0000E-07	1.0000E-05	1.0000E-04
$X_{E,0}$							
$A_p \delta(r) A_p$	6.5998E+06	2.2314E+08	2.2279E+08	1.9313E+08	6.7576E+07	2.1868E+07	
$A_p P \delta(r) \cdot PA_p$	1.4222E+04	1.6109E+04	1.6594E+04	6.4354E+04	3.1330E+06	1.9701E+06	7.4519E+05
$A_p P \tilde{V} \cdot PA_p P^{-2} A_p P \delta(r) \cdot PA_p$	-4.1521E+03	-5.1044E+03	-5.1685E+03	-1.1491E+04	-4.1554E+05	-2.5499E+05	-9.8237E+04
$A_p P \delta(r) \cdot PA_p P^{-2} A_p P \tilde{V} \cdot PA_p$	-4.1521E+03	-5.1044E+03	-5.1685E+03	-1.1491E+04	-4.1554E+05	-2.5499E+05	-9.8237E+04
$A_p \tilde{V} A_p P^2 A_p \delta(r) A_p$	-2.7139E+06	-1.6760E+08	-1.6759E+08	-1.6730E+08	-1.4321E+08	-4.4639E+07	-1.2118E+07
$A_p \delta(r) A_p P^2 A_p \tilde{V} A_p$	-2.7139E+06	-1.6760E+08	-1.6759E+08	-1.6730E+08	-1.4321E+08	-4.4639E+07	-1.2118E+07
$-A_p P \tilde{V} \cdot PA_p A_p \delta(r) A_p$	6.3791E+05	2.7267E+07	2.7267E+07	2.7222E+07	2.3458E+07	7.8427E+06	2.3461E+06
$-A_p \delta(r) A_p A_p P \tilde{V} \cdot PA_p$	6.3791E+05	2.7267E+07	2.7267E+07	2.7222E+07	2.3458E+07	7.8427E+06	2.3461E+06
$-A_p \tilde{V} A_p A_p P \delta(r) \cdot PA_p$	2.7099E+03	2.9874E+03	3.4073E+03	4.4780E+04	2.7008E+06	1.6020E+06	5.5531E+05
$-A_p P \delta(r) \cdot PA_p A_p \tilde{V} A_p$	2.7099E+03	2.9874E+03	3.4073E+03	4.4780E+04	2.7008E+06	1.6020E+06	5.5531E+05
$W_1^2 (A_p \delta(r) A_p + A_p P \delta(r) \cdot PA_p)$	-1.9578E+05	-3.3906E+07	-3.3905E+07	-3.3850E+07	-2.9024E+07	-7.5274E+06	-1.5336E+06
$(A_p \delta(r) A_p + A_p P \delta(r) \cdot PA_p) W_1^2$	-1.9578E+05	-3.3906E+07	-3.3905E+07	-3.3850E+07	-2.9024E+07	-7.5274E+06	-1.5336E+06
$W_1 (A_p \delta(r) A_p + A_p P \delta(r) \cdot PA_p) W_1$	6.5323E+05	8.8248E+07	8.8247E+07	8.8107E+07	7.5937E+07	2.0968E+07	4.6564E+06
$W_2 A_p P \delta(r) \cdot PA_p$	5.0771E+02	7.4469E+02	4.1668E+02	-3.1906E+04	-2.0953E+06	-1.1125E+06	-3.1912E+05
$A_p P \delta(r) \cdot PA_p W_2$	5.0771E+02	7.4469E+02	4.1668E+02	-3.1906E+04	-2.0953E+06	-1.1125E+06	-3.1912E+05
$W_2 A_p \delta(r) A_p$	8.3715E+05	1.1117E+08	1.1116E+08	1.1095E+08	9.3355E+07	2.4797E+07	5.3022E+06
$A_p \delta(r) A_p W_2$	8.3715E+05	1.1117E+08	1.1116E+08	1.1095E+08	9.3355E+07	2.4797E+07	5.3022E+06
$\Sigma X_{E,0}$	6.6140E+06	2.2316E+08	2.2316E+08	2.2285E+08	1.9626E+08	6.9546E+07	2.2613E+07
$X_{E,1}$	-4.1548E+06	-2.8066E+08	-2.8065E+08	-2.8010E+08	-2.3494E+08	-7.0898E+07	-1.8630E+07
$X_{E,2}$	1.9370E+06	2.4277E+08	2.4276E+08	2.4225E+08	2.0041E+08	5.3282E+07	1.1555E+07

The terms are labeled following the notation used in the references of Wolf and Reiher [33] and of Bucinsky et al. [39]

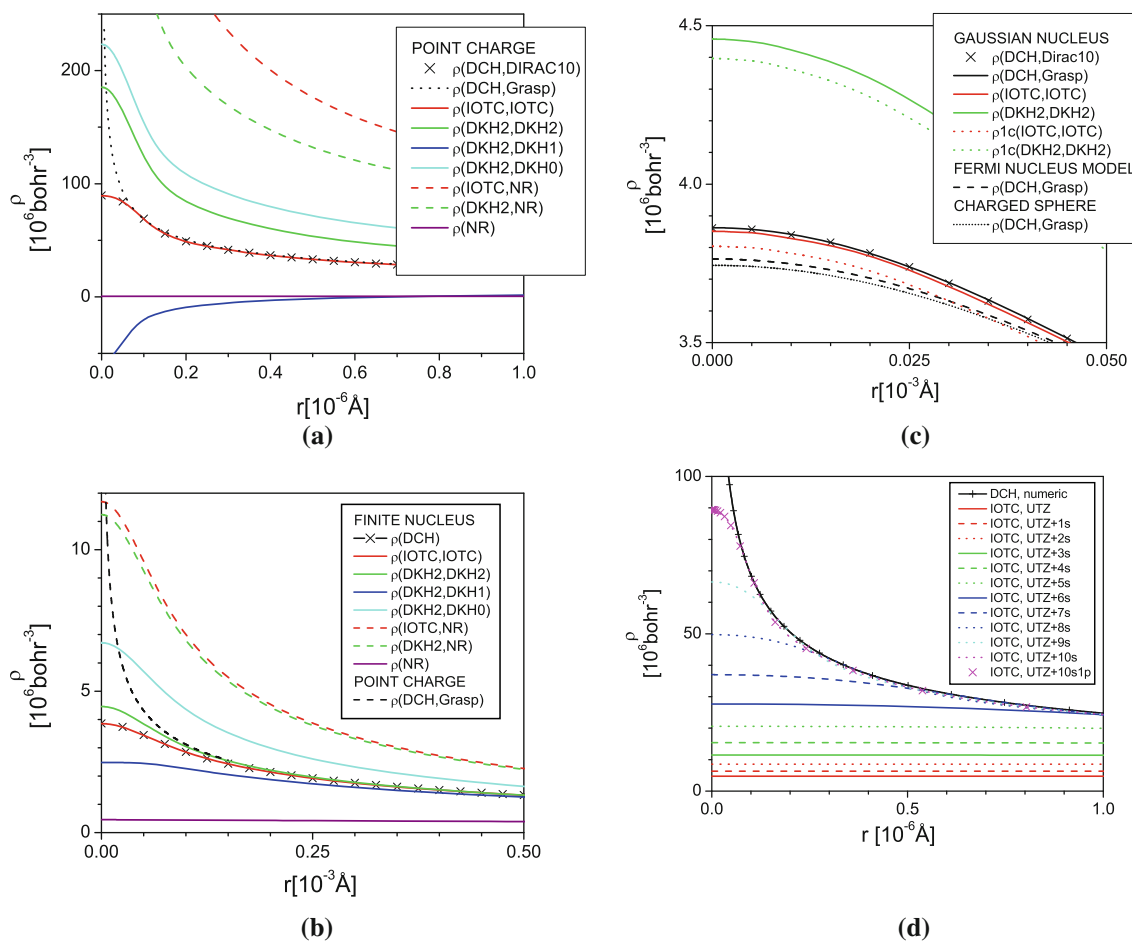


Fig. 1 Radial distributions of total electron densities of radon atom, if not otherwise stated the UTZ+10s basis set has been employed. **a** Point charge nucleus. **b** Gaussian charge distribution model of nucleus.

nucleus. **c** Comparison of finite nucleus models. **d** The basis set artifact $\rho(\text{IOTC}, \text{UTZ}+\text{NsMp})$ basis set series, point charge nucleus

the nucleus as in the case of the point charge nucleus model (see Table 3 and Fig. 1b, c). This means that the PCE corrected 2c-IOTC electron density yields the best agreement with the DCH density. The $\rho(\text{DKH2,DKH2})$ contact density is overestimated in comparison with the $\rho(\text{IOTC}, \text{IOTC})$ density and is in a better agreement with $\rho(\text{IOTC}, \text{IOTC})$ than the $\rho(\text{DKH2,DKH1})$ and the $\rho(\text{DKH2,DKH0})$ densities. The $\rho(\text{DKH2,DKH1})$ contact density is not negative, the contributions of the negative $X_{E,1}$ terms are smaller than in the case of the point charge nucleus model, see Table 2. In addition, the $\rho(\text{DKH2,DKH1})$ electron density has the maximum localized at the nucleus in the case of the Gaussian nucleus model. It still holds that the $\rho(\text{DKH2,DKH1})$ underestimates the contact density in comparison with $\rho(\text{IOTC}, \text{IOTC})$, and the $\rho(\text{DKH2,DKH0})$ contact density is overestimated and lays approx. in the half between the $\rho(\text{IOTC}, \text{IOTC})$ and $\rho(\text{IOTC}, \text{NR})$ contact densities. The contact density is more sensitive to SO effects in the case of the finite nucleus model comparing to the point charge model nucleus. Furthermore, the

$\rho(\text{DKH2,DKH2})$ as well as the $\rho(\text{DKH2,DKH1})$ densities are in a better agreement with the DCH density than it is the case for the point charge nucleus model. The PCE error is very large also for the Gaussian charge distribution model of nucleus and overestimates the electron density at the nucleus by almost a factor of three. It holds that PCE is for the UTZ+10s basis set larger at the IOTC level than at the DKH2 level of theory, see Table 3.

The DCH contact densities of different finite nucleus models are presented in Table 3 and in Fig. 1c. The Gaussian charge distribution model of nucleus leads to a larger contact density in comparison with the Fermi or uniformly charged sphere model of nucleus, see Table 3 [46]. The deviation between the contact densities obtained for the Gaussian and Fermi nucleus models is 2.6%, relative to the Fermi model.

It is noteworthy that the additional p function of the UTZ+10s1p basis set yields in the case of the Gaussian charge distribution model of nucleus the same DCH value of contact density as is the numeric value of contact density

Table 3 The values of the contact density (in bohr^{-3}) of the radon atom for the Gaussian charge distribution nucleus model, if not otherwise stated the quasirelativistic DKH2/IOTC values of electron densities are from the 1-component calculations

Basis	DCH	(IOTC, IOTC)	(DKH2, DKH2)	(DKH2, DKH1)	(DKH2, DKH0)	(IOTC, NR)	(DKH2, NR)	NR
UTZ	3.802284E+06 ^a	3.744273E+06	4.313049E+06	2.424035E+06	6.527944E+06	1.152817E+07	1.103357E+07	4.500066E+05
UTZ+1s	3.867111E+06 ^a	3.808929E+06	4.404161E+06	2.461704E+06	6.620814E+06	1.171591E+07	1.125514E+07	4.499280E+05
UTZ+2s	3.859948E+06 ^a	3.801784E+06	4.393125E+06	2.458732E+06	6.611536E+06	1.169484E+07	1.123783E+07	4.499807E+05
UTZ+3s	3.862843E+06 ^a	3.804672E+06	4.398498E+06	2.457649E+06	6.618370E+06	1.171063E+07	1.125056E+07	4.499485E+05
UTZ+4s	3.861228E+06 ^a	3.803061E+06	4.394859E+06	2.460197E+06	6.611410E+06	1.169501E+07	1.123764E+07	4.499682E+05
UTZ+5s	3.862198E+06 ^a	3.804029E+06	4.397470E+06	2.457321E+06	6.617854E+06	1.170922E+07	1.124958E+07	4.499561E+05
UTZ+6s	3.861606E+06 ^a	3.803438E+06	4.395591E+06	2.459991E+06	6.612368E+06	1.169725E+07	1.123942E+07	4.499635E+05
UTZ+7s	3.861969E+06 ^a	3.803800E+06	4.396936E+06	2.457732E+06	6.616789E+06	1.170683E+07	1.124760E+07	4.499590E+05
UTZ+8s	3.861746E+06 ^a	3.803578E+06	4.395979E+06	2.459543E+06	6.613353E+06	1.169442E+07	1.124125E+07	4.499617E+05
UTZ+9s	3.861883E+06 ^a	3.803714E+06	4.396657E+06	2.458141E+06	6.615956E+06	1.170502E+07	1.124606E+07	4.499601E+05
UTZ+10s	3.861799E+06 ^a	3.803631E+06	4.396179E+06	2.459201E+06	6.614020E+06	1.170086E+07	1.124248E+07	4.499611E+05
UTZ+10s ^b		3.850806E+06	4.457226E+06	2.477015E+06	6.711188E+06	1.169701E+07	1.123899E+07	
UTZ+10s ^c	3.862505E+06 ^a	3.803679E+06	4.396235E+06	2.459245E+06	6.614040E+06	1.170086E+07	1.124248E+07	4.499612E+05
	3.7633807E+06 ^{c,d}							
	3.743804E+06 ^{e,c}							

^a Dirac10 software package^b 2-component DKH2/IOTC values^c Grasp software suite^d Fermi model of nucleus^e Uniformly charged sphere model of nucleus

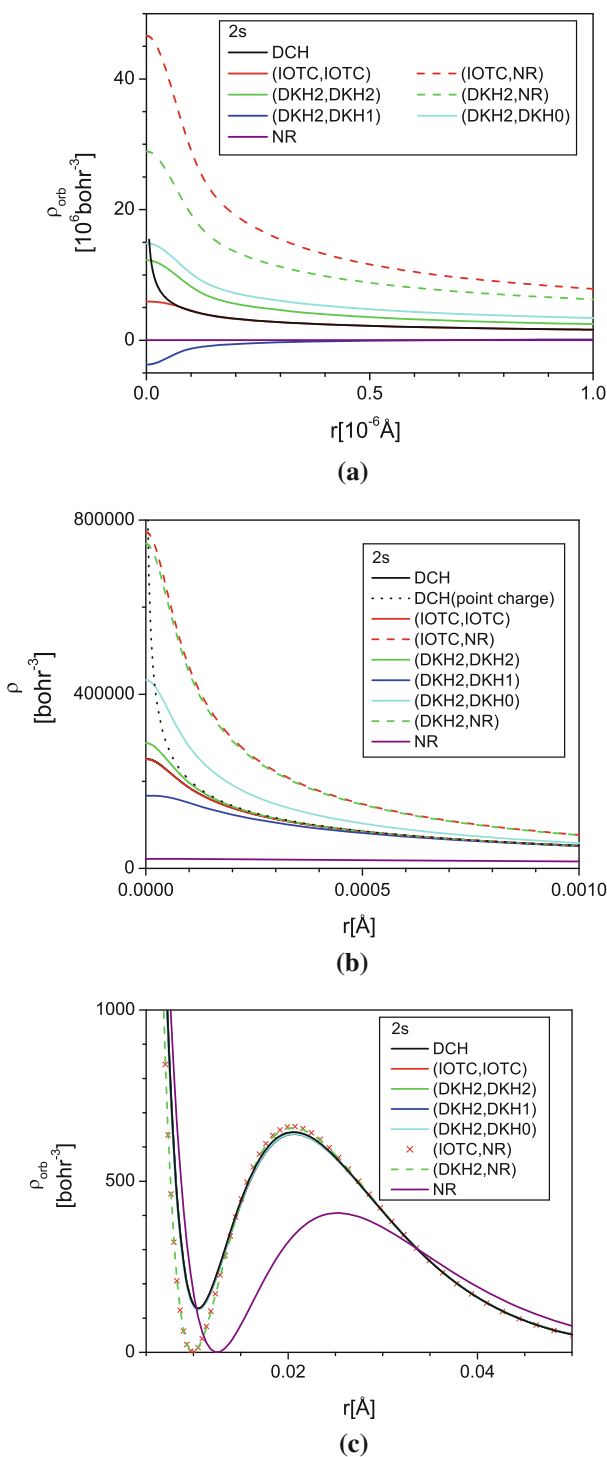


Fig. 2 Radial distributions of 2s orbital densities of radon atom (UTZ+10s basis set). **a** Point charge model of nucleus. **b** Gaussian charge distribution model of nucleus. **c** Local maximum and nodal region

obtained in the Grasp package. On the other hand the UTZ+10s5p DCH contact density, which equals 3.862439×10^6 (not shown in Table 3), is more deviated from the numeric value of DCH contact density than the

UTZ+10s1p contact density, see Table 3. The 1-component $\rho(IOTC,IOTC)$ contact densities calculated in the UDZ and UQZ basis sets ($3.739294 \times 10^{+06}$ and $3.744353 \times 10^{+07}$, respectively) are close to the particular UTZ contact density ($3.744273 \times 10^{+06}$). It is still worth to include at least three tight s Gaussians to yield a more robust value of relativistic contact density of radon atom in the case of the Gaussian model of nucleus, see Table 3. On the other hand, the NR calculation of contact density is very little sensitive to inclusion of tight Gaussians into the UTZ basis set; nevertheless, this value is not reliable in the sense of the importance of relativistic effects.

3.2 s Orbitals

The radial distributions of the canonical HF s orbital densities of the radon atom (UTZ+10s basis set) are presented in Fig. 2 (the 2s orbital has been chosen as a representative). Figure 2a is presenting the radial distribution of the 2s orbital density in the vicinity of the point charge nucleus. Figure 2b presents the radial distribution of the 2s orbital density in the vicinity of the Gaussian charge distribution model of nucleus. Figure 2c presents the radial distributions of the 2s orbital density in the region of the second maximum and the node of the NR 2s orbital density. The contact densities of all the s orbitals of Rn (UTZ+N_s basis sets) are shown in Tables 4 and 5. Although in Fig. 2 are presented only the radial distributions of the 2s orbital densities, the relativistic effects and PCE in the remaining s orbitals are qualitatively the same (not shown).

In general and/or independent of the nucleus model (finite size nucleus or point charge), the s orbitals have the largest contribution to PCE and to the (scalar/spinfree) relativistic effects in the total electron density of the radon atom (see Tables 1 and 3) [39]. Thus, the conclusions about the relativistic effects and PCE in the total electron density are quantitatively and qualitatively valid also for the s orbitals. This means that, the PCE contaminated DKH2/IOTC radial distributions of 2s orbital densities [$\rho_{2s}(IOTC,NR)$ and $\rho_{2s}(DKH2,NR)$, see Fig. 2a, b], are obviously overestimated at the nucleus (what causes the same features in the appropriate PCE contaminated total electron densities) [39]. Besides, the PCE contaminated s orbitals are not nodeless (see Fig. 2c), which is the second important feature of PCE for all orbitals in general.

Although the limiting behavior of the contact density of the relativistic s orbitals is determined by the choice of the nucleus, the agreement between the radial distributions of the PCE corrected $\rho_{2s}(IOTC,IOTC)$ and $\rho_{2s}(DCH)$ orbital densities at the finite basis set level of theory is very good for both the point charge and Gaussian charge distribution model of nucleus (besides the issue of the basis set artifact

Table 4 Contact s orbital density (finite basis set approach) for the point charge model of nucleus, using the UTZ+10s basis set (density is in a.u., i.e., bohr^{-3})

Approach	1s	2s	3s	4s	5s	6s
DCH	3.700562E+07	5.948800E+06	1.393323E+06	3.633850E+05	8.027550E+04	1.201789E+04
2c-(IOTC, IOTC)	3.689500E+07	5.930536E+06	1.389632E+06	3.625151E+05	8.009117E+04	1.198960E+04
1c-(IOTC, IOTC)	3.690477E+07	5.934874E+06	1.390494E+06	3.624814E+05	7.994347E+04	1.191615E+04
2c-(DKH2,DKH2)	7.653766E+07	1.225261E+07	2.870134E+06	7.486637E+05	1.653412E+05	2.471481E+04
1c-(DKH2,DKH2)	7.655682E+07	1.226100E+07	2.871812E+06	7.485787E+05	1.650311E+05	2.455879E+04
2c-(DKH2,DKH1)	-2.385617E+07	-3.734511E+06	-8.716961E+05	-2.271816E+05	-5.016329E+04	-7.498139E+03
1c-(DKH2,DKH1)	-2.386201E+07	-3.737037E+06	-8.721958E+05	-2.271541E+05	-5.007052E+04	-7.451214E+03
2c-(DKH2,DKH0)	9.208503E+07	1.483561E+07	3.478607E+06	9.075987E+05	2.004540E+05	2.996373E+04
1c-(DKH2,DKH0)	9.210823E+07	1.484581E+07	3.480653E+06	9.074985E+05	2.000782E+05	2.977453E+04
2c-(IOTC,NR)	2.934364E+08	4.662154E+07	1.090470E+07	2.843483E+06	6.281586E+05	9.403412E+04
1c-(IOTC,NR)	2.935528E+08	4.666113E+07	1.091271E+07	2.843544E+06	6.270719E+05	9.346883E+04
2c-(DKH2,NR)	1.791079E+08	2.892940E+07	6.785820E+06	1.770640E+06	3.910760E+05	5.845802E+04
1c-(DKH2,NR)	1.791531E+08	2.894934E+07	6.789820E+06	1.770447E+06	3.903433E+05	5.808896E+04
NR	1.998306E+05	2.234202E+04	5.114915E+03	1.324003E+03	2.863373E+02	3.882039E+01

Table 5 Contact s orbital density (finite basis set approach) for the Gaussian charge distribution model of nucleus, using the UTZ+10s basis set (density is in a.u., i.e., bohr^{-3})

Approach	1s	2s	3s	4s	5s	6s
DCH	1.570936E+06	2.516291E+05	5.891179E+04	1.536284E+04	3.393197E+03	5.076623E+02
2c-(IOTC, IOTC)	1.566270E+06	2.508654E+05	5.875773E+04	1.532665E+04	3.385650E+03	5.065176E+02
1c-(IOTC, IOTC)	1.566695E+06	2.510484E+05	5.879408E+04	1.532523E+04	3.379406E+03	5.034075E+02
2c-(DKH2,DKH2)	1.814018E+06	2.878090E+05	6.733522E+04	1.755883E+04	3.877100E+03	5.792531E+02
1c-(DKH2,DKH2)	1.814467E+06	2.880048E+05	6.737429E+04	1.755682E+04	3.869873E+03	5.756042E+02
2c-(DKH2,DKH1)	1.004460E+06	1.668862E+05	3.931438E+04	1.026910E+04	2.268455E+03	3.389462E+02
1c-(DKH2,DKH1)	1.004720E+06	1.670036E+05	3.933820E+04	1.026819E+04	2.264286E+03	3.368201E+02
2c-(DKH2,DKH0)	2.732133E+06	4.325349E+05	1.011542E+05	2.637505E+04	5.823625E+03	8.700666E+02
1c-(DKH2,DKH0)	2.732808E+06	4.328286E+05	1.012127E+05	2.637198E+04	5.812759E+03	8.645845E+02
2c-(IOTC,NR)	4.836528E+06	7.721303E+05	1.807392E+05	4.713775E+04	1.041230E+04	1.557742E+03
1c-(IOTC,NR)	4.837814E+06	7.726912E+05	1.808505E+05	4.713325E+04	1.039306E+04	1.548173E+03
2c-(DKH2,NR)	4.642001E+06	7.456000E+05	1.747401E+05	4.558542E+04	1.006661E+04	1.504023E+03
1c-(DKH2,NR)	4.643163E+06	7.461116E+05	1.748426E+05	4.558048E+04	1.004791E+04	1.494558E+03
NR	1.963752E+05	2.195750E+04	5.027011E+03	1.301261E+03	2.814232E+02	3.815572E+01

for the point charge nucleus). The $\rho_{2s}(DKH2,DKH1)$ orbital density yields a negative electron density (as is the case for the total electron density) for the point charge nucleus model if tight enough gaussians are included in the basis set, see the UTZ+10s values of contact densities of all the $s(DKH2,DKH1)$ orbitals in Table 4. The $\rho_{2s}(DKH2,DKH2)$ orbital density is also considerably shifted from the nucleus for the point charge model of nucleus and is quite close to the $\rho_{2s}(DKH2,DKH0)$ orbital density, see Fig. 2a and the values of the DKH2 s orbital contact densities in Table 4. On the other hand, the $\rho_{2s}(DKH2,DKH1)$ orbital density in the presence of the Gaussian charge distribution model is not negative (same holds for the particular

electron density) and the behavior of the $\rho_{2s}(DKH2,DKH2)$ orbital density is improved comparing to the $\rho_{2s}(DCH)$ in the case of the Gaussian charge distribution model, see Fig. 2b. In addition, the PCE corrected DKH2/IOTC ρ_{2s} (independent of nucleus model) are nodeless and do agree with the DCH 2s orbital density (even for the lower order PCE corrected DKH2 orbital densities), see Fig. 2c.

The 1-component/scalar (1c) and 2-component (2c) quasirelativistic radial distributions of 2s orbital densities are very similar [1c quasirelativistic orbital densities are not shown in Fig. 2a–c, but see the values of the contact density in Tables 4 and 5], *i.e.* the SO effects do not cause a significant redistribution of the s orbital electron density.

Hence, the difference in the values of the PCE corrected 1-component and 2-component DKH2/IOTC total electron densities in the vicinity of nucleus is not caused by the s orbitals (see the following p orbital section). The 1-component and 2-component s orbital contact densities (see Tables 4 and 5) do not deviate by more than 1% from each other when using the UTZ+10s basis set. Furthermore, the nodal behavior is correctly assessed also for the scalar s orbitals, i.e. the PCE corrected 1c IOTC/DKH2 orbital densities are nodeless (not shown), while the PCE contaminated scalar IOTC/DKH2 orbital densities contain nodes (not shown), as is the case for the 2-component PCE contaminated s orbital densities.

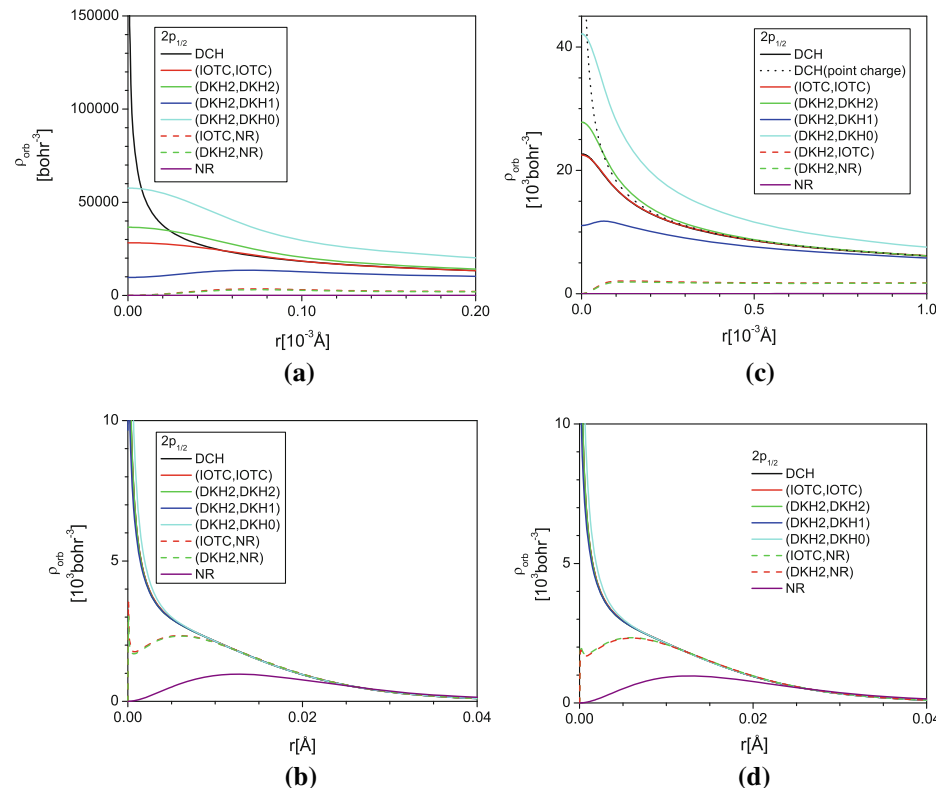
The non-relativistic s contact density is underestimated for the Gaussian charge distribution model of nucleus by almost a factor of 10 (see Fig. 2a, c). Furthermore, the non-relativistic density distribution is more diffuse comparing to the relativistic one, *i.e.* the relativistic contraction of the s orbitals is obvious.

3.3 p Orbitals

Although the s orbitals have the largest contribution to the relativistic effects and PCE in the electron density in the vicinity of nucleus, the orbitals of the remaining angular symmetry might not be forgotten (whether scalar p , d , f or SO-splittered $p_{1/2}$, $p_{3/2}$, $d_{3/2}$, $d_{5/2}$, $f_{5/2}$ and $f_{7/2}$). The higher

angular symmetry orbitals are still involved in chemical bonding and are of significance by means of direct or indirect relativistic effects in the total electron density and by means of SO splitting [1]. In the case of the p orbitals, the SO-splittered $2c/4c p_{1/2}$ and $p_{3/2}$ orbitals have a different behavior [3, 4]. In the case of the p orbitals, the radial distributions of the $2p$, $2p_{1/2}$ and $2p_{3/2}$ orbitals are considered more closely; the nodal behavior is discussed for the $3p$, $3p_{1/2}$ and $3p_{3/2}$ orbitals, see Figs. 3, 4 and 5. Figure 3a, c present the radial distribution of the $2p_{1/2}$ orbital density obtained at the DCH, IOTC, and DKH2 levels of theory for the point charge and Gaussian charge distribution models of nucleus, respectively. Figure 3b, d present the radial distribution of the $2p_{1/2}$ orbital density in the vicinity of nucleus for the point charge and Gaussian charge distribution model of nucleus, respectively. The $2p_{3/2}$ orbitals are presented in Fig. 4a. Figure 4b shows the nodal behavior of the DCH, IOTC, and NR $3p_{1/2}$, $3p_{3/2}$ and $3p$ orbitals. The radial distributions of scalar $2p$ orbital densities are, in more detail, presented in Fig. 5. In Tables 6 and 7 are summarized the values of contact density of DCH and PCE corrected IOTC/DKH2 p and $p_{1/2}$ orbitals. The PCE contaminated IOTC and DKH2 p and $p_{1/2}$ orbitals as well as the NR one have zero density at nucleus; thus, these are omitted from Tables 6 and 7. Table 8 presents the contact densities of the (IOTC, IOTC) and (DKH2, DKH1) $2p_{1/2}$ and $2p$ orbitals using the point

Fig. 3 Radial distributions of the relativistic $2p_{1/2}$ and NR $2p$ orbital densities of radon atom (UTZ+10s basis set). **a** Point charge nucleus. **b** Detail for point charge nucleus. **c** Gaussian charge model of nucleus. **d** Detail for Gaussian charge model of nucleus



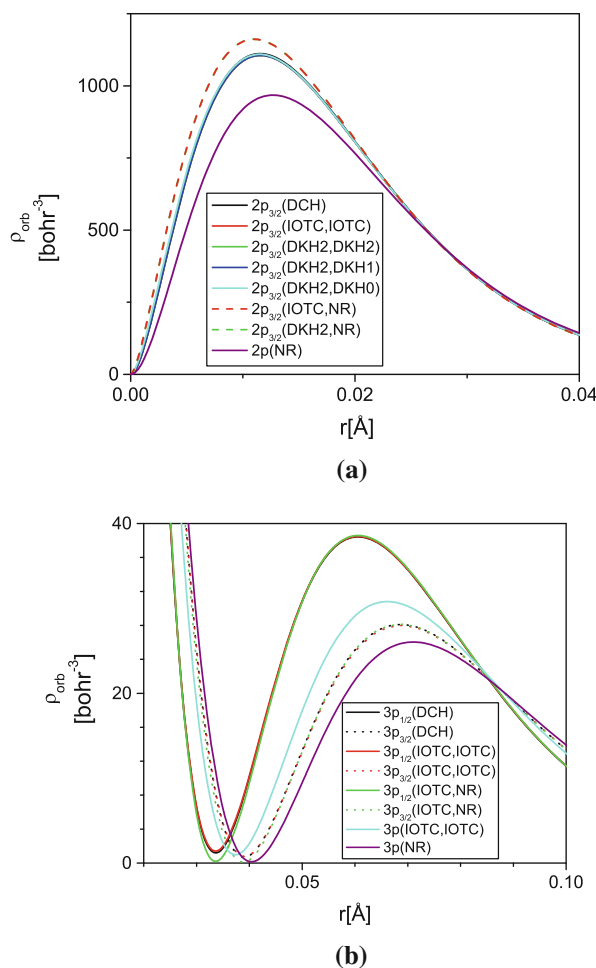


Fig. 4 Radial distributions of the $3p_{3/2}$ orbitals and the region of the NR node of the $3p$ orbital of radon atom (UTZ+10s basis set). **a** $2p_{3/2}$ orbitals, point charge nucleus. **b** $3p_{1/2}$, $3p_{3/2}$ and $3p$ orbitals in the region of the NR node

charge model of nucleus and the UTZ+10sMp basis sets (where $M = 1, \dots, 5$).

In comparison with s orbitals is the SO splitting the most significant relativistic feature of the p orbitals, giving rise to the $p_{1/2}$ and $p_{3/2}$ orbitals. Furthermore, the $p_{1/2}$ orbitals have a non-zero contact density because of the s character [1, 3, 4]. Hence, the radial distributions of the electron density of the 4c and PCE corrected 2c $p_{1/2}$ orbitals is very similar to the s orbitals (see Fig. 3a, d), while the $p_{3/2}$ orbitals have a similar radial distribution like the non-relativistic p orbitals, see Fig. 4a.

The PCE corrected $2p_{1/2}(\text{IOTC,IOTC})$ orbital density agrees well with the DCH $2p_{1/2}$ orbital density (numeric as well as finite basis set) in the case of the Gaussian charge distribution model of nucleus, see Fig. 3b, d. Although the basis set artifact is present in the case of the point charge nucleus model when comparing the numeric DCH and finite basis set (IOTC, IOTC) $2p_{1/2}$ orbital densities (see

Fig. 2a), the contact density of the finite basis set DCH and (IOTC, IOTC) calculations are deviated by less than 1% from each other. The quite significant basis set artifact in the case of the $2p_{1/2}$ orbitals is caused by the missing tight p functions in the UTZ+10s basis set (see Table 8). It is noteworthy that the UTZ+10s contact density of the $2p_{1/2}(\text{IOTC,IOTC})$ orbital in the case of the point charge model of nucleus (see Table 6) is significantly smaller than for the UTZ basis set (see Table 8).

The PCE corrected $2p_{1/2}(\text{DKH2,DKH2})$ orbital density is overestimated at the nucleus in comparison with the PCE corrected IOTC and/or the DCH $2p_{1/2}$ orbitals (see Fig. 3a, c and Table 6 and 7) in a similar way like is found in the case of the s orbitals (or total electron density), see Fig. 2a. Nevertheless, the deviation of the $2p_{1/2}(\text{DKH2,DKH2})$ orbital density (UTZ+10s basis set) from the $2p_{1/2}(\text{DCH})$ orbital density (Fig. 3a) is in the case of the point charge nucleus smaller than in the case of the total electron density (Fig. 1a) or the density of the $2s$ orbital (Fig. 2a). The lower order PCE corrected $2p_{1/2}(\text{DKH2,DKH1})$ orbital density, independent of the nucleus model, has the maximum density shifted away from the nucleus and the $2p_{1/2}(\text{DKH2,DKH1})$ contact density is underestimated in comparison with the particular finite basis set DCH value of contact density, see Fig. 3a, c and Tables 6, 7, but it is not found negative in the case of the UTZ+10s basis set. Furthermore, the $2p_{1/2}(\text{DKH2,DKH1})$ and $2p(\text{DKH2,DKH1})$ contact densities are becoming larger with the number of tight p Gaussians of the UTZ+10sMp basis set, see Table 8. The radial distribution of the $2p_{1/2}(\text{DKH2,DKH0})$ orbital density is overestimated compared to the $2p_{1/2}(\text{DCH})$ density distribution, see Fig. 3a, c, which is again exactly the same feature as found for the particular total electron or s orbital densities.

The PCE contaminated $2p_{1/2}(\text{IOTC,NR})$ and $2p_{1/2}(\text{DKH2,NR})$ orbital densities, as already mentioned, are not overestimated at nucleus, like in the case of the PCE contaminated IOTC/DKH2 s orbitals, but are actually zero at the nucleus, see Fig. 3a, c as well as Fig. 5c, d. Although in Fig. 3b, d it rather seems that the PCE contaminated $2p_{1/2}$ electron densities are non-zero at nucleus, the closer look shows that the PCE contaminated radial distributions of the quasirelativistic IOTC/DKH2 $2p_{1/2}$ orbital electron densities are very steep at the nucleus and contain a local maximum of electron density close to the nucleus, see Figs. 3a, c and 5b, d. This local maximum in the PCE contaminated $p_{1/2}$ orbital densities is much sharper and larger in value in the case of the point charge nucleus model (Fig. 5b) compared to the Gaussian charge model of nucleus (Fig. 5d). The PCE contaminated $2p_{1/2}$ orbital density distributions start to agree with the PCE corrected one in the region of the maximum of the NR $2p$ orbital density (at approx. 0.01 \AA), see Fig. 5b, d.

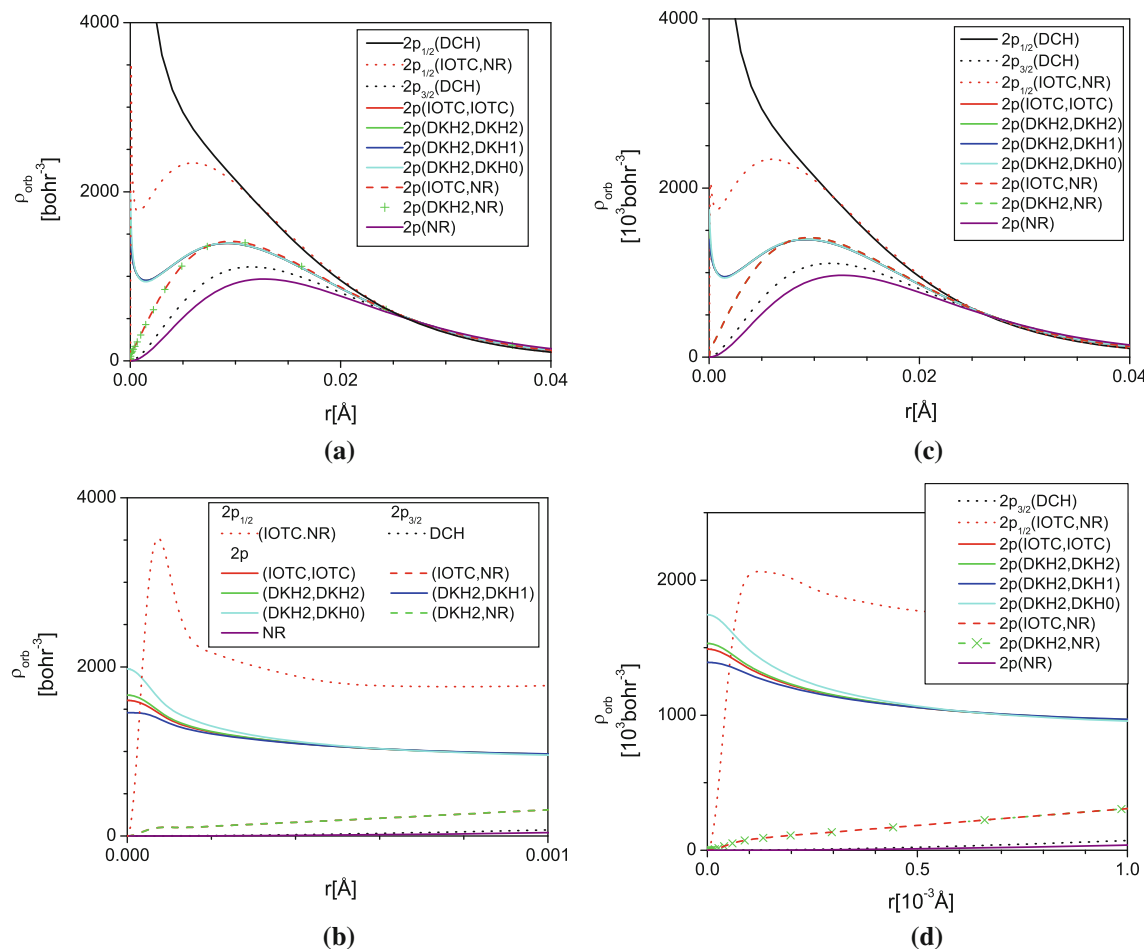


Fig. 5 Details of the radial distributions of the scalar $2p$ orbital densities of radon atom (UTZ+10s basis set). **a** Point charge nucleus. **b** Detail for point charge nucleus. **c** Gaussian model of nucleus. **d** Detail for Gaussian model of nucleus

Table 6 The relativistic contact densities (finite basis set approach) of p and $p_{1/2}$ orbitals of radon atom for the point charge nucleus using the UTZ+10s basis set (density is in a.u., i.e. bohr^{-3})

Approach	$2p_{1/2}$	$3p_{1/2}$	$4p_{1/2}$	$5p_{1/2}$	$6p_{1/2}$
DCH	28,156.1152	7,421.9498	1,923.9734	392.5579	46.2420
2c-(IOTC, IOTC)	28,278.8006	7,453.7408	1,933.2253	394.7706	46.6175
1c-(IOTC, IOTC)	1,603.4756	435.9578	113.5038	22.7062	2.4057
2c-(DKH2,DKH2)	36,595.4382	9,607.6829	2,489.5464	508.1345	59.9400
1c-(DKH2,DKH2)	1,665.8476	453.1137	117.9751	23.6012	2.5006
2c-(DKH2,DKH1)	9,657.7732	2,608.9822	680.5548	139.1332	16.4178
1c-(DKH2,DKH1)	1,457.1684	396.0951	103.1268	20.6305	2.1859
2c-(DKH2,DKH0)	57,607.5096	15,144.8744	3,925.5934	801.3031	94.5236
1c-(DKH2,DKH0)	1,975.6210	538.0939	140.1269	28.0340	2.9703

The scalar PCE corrected $2p(\text{IOTC},\text{IOTC})$ and $2p(\text{DKH2},\text{DKH2})$ orbitals (see Fig. 5b, d) have non-zero density at nucleus; furthermore, they have the character of both the $2p_{1/2}$ (non-zero density at nucleus, see Tables 6 and 7) and the $2p_{3/2}$ orbitals (a maximum in the orbital density distribution like the $2p(\text{NR})$ orbital), see Fig. 5a, c. The

differences in the radial distributions of the scalar DKH2/IOTC $2p$ electron densities in the vicinity of the nucleus are similar to the particular $p_{1/2}$ orbital densities, see Figs. 3, 5. The $2p(\text{DKH2},\text{DKH2})$ orbital density is the most close to the $2p(\text{IOTC},\text{IOTC})$ density (which is taken as reference in this case). The $2p(\text{DKH2},\text{DKH0})$ orbital density is

Table 7 The relativistic contact density (finite basis set approach) of p and $p_{1/2}$ orbitals of radon atom for the Gaussian charge distribution nucleus model, using the UTZ+10s basis set (density is in a.u., i.e. bohr^{-3})

Approach	$2p_{1/2}$	$3p_{1/2}$	$4p_{1/2}$	$5p_{1/2}$	$6p_{1/2}$
DCH	22,383.0987	5,898.0544	1,528.8077	311.9204	36.7407
2c-(IOTC, IOTC)	22,480.6009	5,923.3143	1,536.1585	313.6783	37.0390
1c-(IOTC, IOTC)	1,489.6587	404.9752	105.4349	21.0920	2.2347
2c-(DKH2,DKH2)	27,811.3207	7,300.8451	1,891.7585	386.1173	45.5449
1c-(DKH2,DKH2)	1,531.3011	416.4594	108.4289	21.6913	2.2983
2c-(DKH2,DKH1)	11,062.5732	2,960.8631	770.6884	157.4765	18.5796
1c-(DKH2,DKH1)	1,391.2191	378.1539	98.4534	19.6956	2.0868
2c-(DKH2,DKH0)	42,118.0071	11,063.5012	2,867.1244	585.2135	69.0298
1c-(DKH2,DKH0)	1,744.1964	475.0520	123.7084	24.7493	2.6223

Table 8 The values of the (IOTC, IOTC) and (DKH2,DKH1) contact densities of the $2p_{1/2}$ and $2p$ orbitals (UTZ, UTZ+10sMp basis sets) for the point charge model of nucleus

	$2p_{1/2}(\text{IOTC},\text{IOTC})$	$2p(\text{IOTC},\text{IOTC})$	$2p_{1/2}(\text{DKH2},\text{DKH1})$	$2p(\text{DKH2},\text{DKH1})$
UTZ	28,279.1	1,603.3	9,657.8334	1,457.1753
UTZ+10s1p	37,672.9	1,769.3142	29,068.8872	1,554.9850
UTZ+10s2p	50,399.9	1,953.9274	34,746.1390	1,653.5727
UTZ+10s3p	67,062.8	2,151.4422	40,320.0280	1,747.5700
UTZ+10s4p	89,567.3	2,372.8685	45,383.1360	1,842.0645
UTZ+10s5p	119,159.0	2,611.0643	48,460.1175	1,930.6996

overestimated at the nucleus, and the $2p(\text{DKH2},\text{DKH1})$ electron density is underestimated in comparison with the scalar $2p(\text{IOTC},\text{IOTC})$ orbital density as is the case in the quasirelativistic $2p_{1/2}$ orbital densities. The maximum of the scalar $2p(\text{DKH2},\text{DKH1})$ orbital density distribution is localized on the nucleus. There is no significant difference found between the PCE contaminated scalar $2p(\text{IOTC},\text{NR})$ and $2p(\text{DKH2},\text{NR})$ orbital densities which are overlapping, see Fig. 5. Similar to the density distribution of the PCE contaminated $2p_{1/2}(\text{DKH2},\text{NR})$ and $2p_{1/2}(\text{IOTC},\text{NR})$ orbitals, the PCE contaminated scalar $2p(\text{DKH2},\text{NR})/2p(\text{IOTC},\text{NR})$ orbitals have zero density at nucleus and quite an ordinary p character. However, Fig. 5c, d show on an irregularity in the PCE contaminated $2p(\text{DKH2},\text{NR})$ and $2p(\text{IOTC},\text{NR})$ orbital density distributions close to the nucleus with an almost zero slope, see Fig. 5b, d.

In general, the difference between the PCE corrected quasirelativistic DKH2/IOTC 2-component $p_{1/2}$ and the scalar p orbital density distributions has the dominant contribution to the difference of the PCE corrected 1-component and 2-component DKH2/IOTC total electron densities at and close to the nucleus, see Tables 1, 3, 4, 5, 6 and 7 [39]. On the other hand, the PCE contaminated DKH2/IOTC contact densities of the $p_{1/2}$ and p orbitals are zero, hence the PCE contaminated 1- and 2-component DKH2/IOTC contact densities are much less deviated from

each other, i.e. only the s orbitals contribute to the difference of the 1- and 2-component PCE contaminated DKH2/IOTC total electron densities, see Tables 1, 3, 4 and 5.

The $p_{3/2}$ orbitals (as well as the following higher angular symmetry orbitals) are less affected by PCE as well as relativistic effects compared to the s and $p_{1/2}$ orbitals. The PCE contaminated $2p_{3/2}(\text{IOTC},\text{NR})$ and $2p_{3/2}(\text{DKH2},\text{NR})$ orbitals are overestimating the electron density in the vicinity of the nucleus and in the region of the maximum of the $2p_{3/2}$ density distribution comparing to PCE corrected IOTC, DKH2 or the DCH orbital densities, i.e. $2p_{3/2}(\text{IOTC},\text{NR})$ and $2p_{3/2}(\text{DKH2},\text{NR})$ densities are laying above the $2p_{3/2}(\text{DCH})$ and the PCE corrected quasirelativistic $2p_{3/2}(\text{IOTC},\text{IOTC})/2p_{3/2}(\text{DKH2},\text{DKH2})$ curves, see Fig. 4a. The radial distributions of the $2p_{3/2}(\text{DKH2},\text{DKH1})$ and $2p_{3/2}(\text{DKH2},\text{DKH0})$ orbital densities yield a considerable agreement with the radial distribution of the DCH $2p_{3/2}$ orbital density as well. Although it has to be pointed out that the local maximum of the PCE corrected $p_{3/2}(\text{IOTC},\text{IOTC})$ [as well as $p_{1/2}(\text{IOTC},\text{IOTC})$] orbital density is slightly underestimated[overestimated] compared to the radial distribution of the particular DCH orbital densities, which is hard to see in Fig. 5c (holds also for the DKH2 PCE corrected orbital densities). This is shown and discussed in more detail for the case of the d and f orbitals (see the particular sections).

Besides the discussed behavior of the electron density distributions at the nucleus, the nodal behavior of the PCE corrected and contaminated DKH2/IOTC $p_{1/2}$, $p_{3/2}$ and p orbital densities is worth to be mentioned, see Fig. 4b. The PCE corrected $3p_{1/2}(IOTC,IOTC)$ and $3p_{3/2}(IOTC, IOTC)$ orbital densities do correctly assess the nodal (i.e. nodeless) behavior of the SO-splitted p orbital densities in comparison with the particular DCH orbital densities, see Fig. 4b. In addition, the 1-component PCE corrected $3p(IOTC,IOTC)$ orbital (see Fig. 5c) density is nodeless as well. The 1c and 2c PCE contaminated IOTC $p(IOTC,NR)$ orbital densities are zero in the nodes, see Fig. 5c. The DKH2 p orbital densities (not shown) have the same features in the nodes as the particular IOTC orbital densities (not shown), i.e. the PCE corrected DKH2 p orbital densities are nodeless (independent of the order of DKH2 PCE correction) while the PCE contaminated $p(DKH2,NR)$ orbitals have nodes.

The non-relativistic $2p$ orbital is found more diffuse (radially expanded) than both $2p_{1/2}$ as well as $2p_{3/2}$ orbital densities (see Figs. 3, 5), i.e. the maximum of the NR $2p$ orbital density is lower than the relativistic one and is shifted outwards from the nucleus comparing to the position of the maximum of the relativistic $2p$ orbital densities.

The presented conclusions and trends of PCE and relativistic effects are valid also for the remaining p orbitals (not shown).

3.4 d Orbitals

The NR/IOTC scalar $3d$ and the IOTC/DCH SO-splitting $3d_{3/2}$ and $3d_{5/2}$ orbital density distributions are presented in Fig. 6, where Fig. 6a shows the region between 0 and 0.2 Å, the details of the radial distributions close to the nucleus are presented in Fig. 6b and the peak (maximum) of the radial distribution is presented in Fig. 6c. There is no discernable impact of the nucleus model for the radial distributions of the $3d$ orbitals (the point charge nucleus model has been used in Fig. 6).

The PCE corrected $3d_{3/2}(IOTC,IOTC)$, $3d_{5/2}(IOTC,IOTC)$ orbital electron densities are overlapping in the nuclear region with the particular DCH orbital densities (see Fig. 6b), though in the region of the maximum (see Fig. 6c) the PCE corrected $3d_{3/2}(IOTC,IOTC)$ density is overestimated compared to the $3d_{3/2}(DCH)$ density; nevertheless, the position of the maximum is the same. On the other hand, the PCE corrected $3d_{5/2}(IOTC,IOTC)$ density is slightly underestimated at the maximum in comparison with $3d_{5/2}(DCH)$ density, see Fig. 6c. These deviations are to be assigned to the PCE associated with the neglected transformation of the 2-electron (electron-electron) Coulomb terms [38, 49].

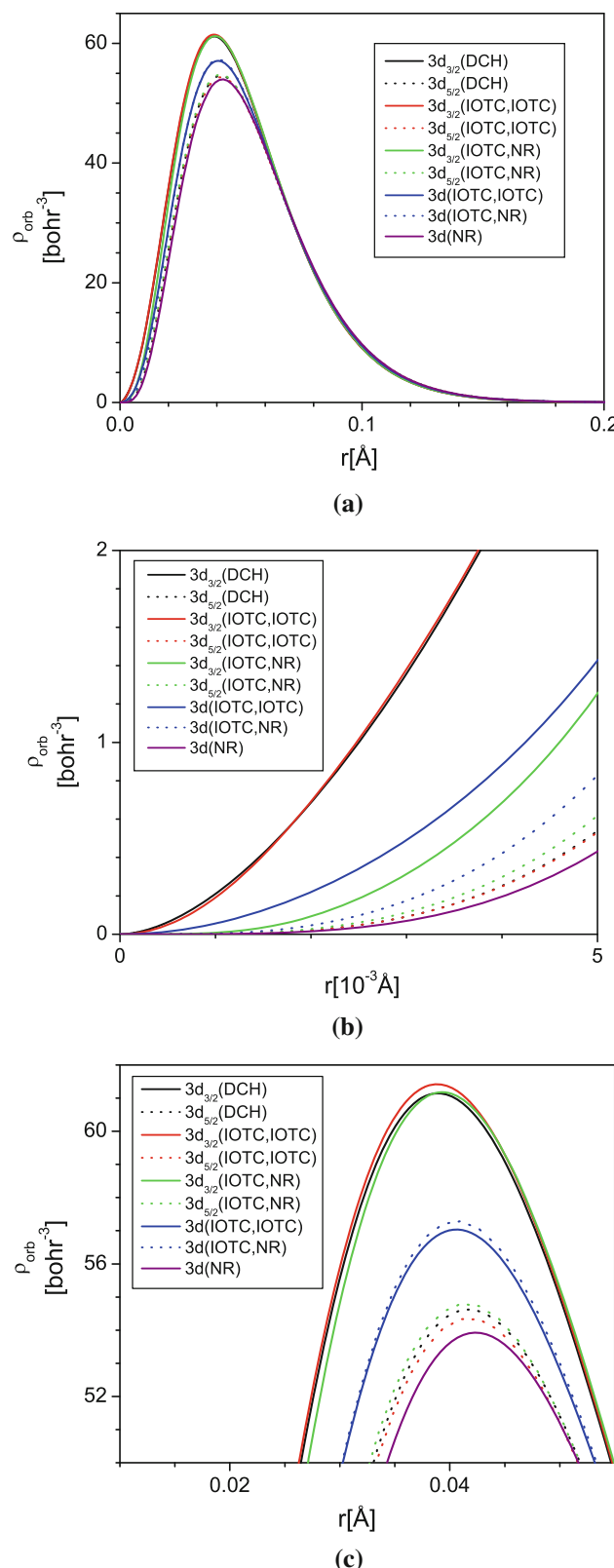


Fig. 6 DCH, IOTC and NR radial distributions of $3d_{3/2}$, $3d_{5/2}$ and $3d$ orbital densities of radon atom (UTZ+10s basis set). **a** Full view. **b** Detail at nucleus. **c** Maximum density, detail

The PCE contaminated $3d_{3/2}(IOTC,NR)$ density is underestimated with respect to the $3d_{3/2}(DCH)$ or $3d_{3/2}(IOTC,IOTC)$ density distribution in the vicinity of the nucleus (see Fig. 6b). The maximum of the $3d_{3/2}(IOTC,NR)$ density is only slightly larger than the maximum of the $3d_{3/2}(DCH)$ electron density distribution (see Fig. 6c), but it is in a closer agreement with the maximum of the $3d_{3/2}(DCH)$ orbital density compared to the PCE corrected $3d_{3/2}(IOTC,IOTC)$ orbital density. The PCE contaminated $3d_{5/2}(IOTC,NR)$ orbital density is overestimated in the vicinity of nucleus (see Fig. 6b) compared to the $3d_{5/2}(DCH)$ density as well as at the maximum of orbital density distribution, see Fig. 6c.

The scalar IOTC $3d$ orbital density lays between the particular $3d_{3/2}$ and $3d_{5/2}$ orbital distributions and can be taken as an SO (degeneracy weighted) average of the $3d_{3/2}$ and $3d_{5/2}$ orbitals, see Fig. 6b. The PCE is only discernable in the vicinity of the nucleus, i.e. the contaminated radial distribution of the $3d(IOTC,NR)$ orbital density is underestimated in the nuclear region in comparison with the PCE corrected one, see Fig. 6c.

Furthermore, the PCE corrected IOTC $4d_{3/2}$, $4d_{5/2}$, $5d_{3/2}$ and $5d_{5/2}$ (as well as scalar $4d/5d$) orbitals are nodeless and overlap with the particular DCH orbital densities in the region of the NR node (not shown). The PCE contaminated $4d_{3/2}$, $4d_{5/2}$, $5d_{3/2}$ and $5d_{5/2}$ orbitals have zero density at nodes; the situation is very similar to the presented nodal behavior of the $2s$ (see Fig. 2c) and $3p$ (see Fig. 4b) orbitals.

Although the DKH2 orbital densities are not shown in Fig. 6, the conclusions about the PCE in the IOTC orbital densities are valid also for the DKH2 orbital densities, i.e. the PCE contaminated DKH2 orbital densities are overlapping with the IOTC one, and the differences between the PCE corrected DKH2 and IOTC densities appear to be marginal even for the lower order PCE corrected DKH2 d orbitals.

The NR $3d$ orbital is more diffuse than the relativistic orbitals ($3d$, $3d_{3/2}$, $3d_{5/2}$), and this holds for the $4d$, $5d$ orbitals as well (not shown). The maximum of the NR $4d$ and $5d$ orbital densities lay next to the maximum of the particular $d_{5/2}(DCH)$ orbitals (not shown).

3.5 f Orbitals

The scalar IOTC or NR $4f$ and the SO-splitted relativistic $4f_{5/2}$ and $4f_{7/2}$ orbital density distributions are presented in Fig. 7. The Figures are presenting the same regions as in the case of the $3d$ orbitals, i.e. Fig. 7a shows the region between 0.0 and 0.4 Å, the radial distributions close to the nucleus are presented in Fig. 7b and the maximum of the radial distribution of the $4f$ orbital is presented in Fig. 7c. There is no discernable impact of the nucleus model on the

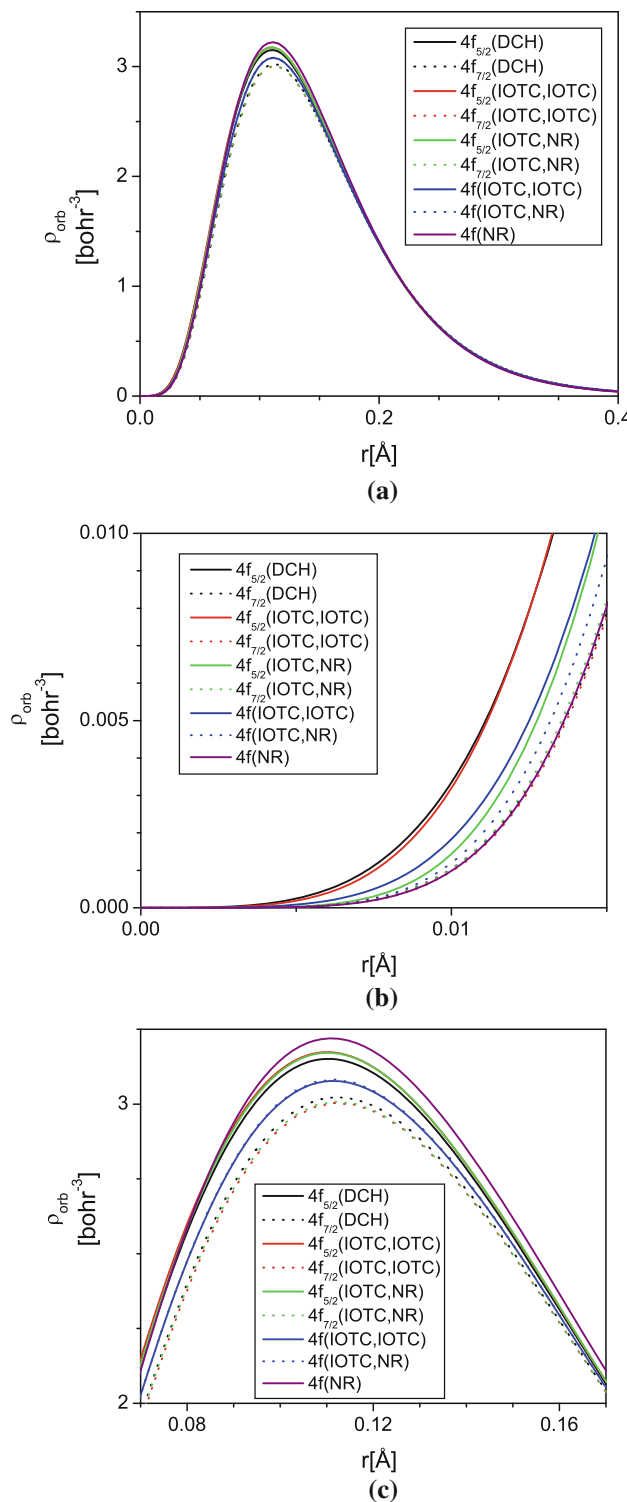


Fig. 7 DCH, IOTC, and NR radial distributions of $4f_{3/2}$, $4f_{5/2}$ and $4f$ orbital densities of radon atom (UTZ+10s basis set). **a** Full view. **b** Detail at nucleus. **c** Maximum density, detail

radial distribution of the $4f$ orbitals (the point charge nucleus model has been used in Fig. 7).

Figure 7a, c show that the maximum of NR $4f$ orbital density is the largest contrary to the s , p and d orbitals.

However, in the nuclear region, the relativistic $4f$ (scalar) and $4f_{5/2}$ electron density distributions are laying above the non-relativistic $4f$ orbital, see Fig. 7b.

The PCE corrected $4f_{5/2}(IOTC,IOTC)$ and $4f_{7/2}(IOTC, IOTC)$ orbital densities are copying the particular DCH orbitals in the vicinity of nucleus, see Fig. 7b. On the other hand, at the maximum of the radial distribution is the PCE corrected $4f_{5/2}(IOTC,IOTC)$ orbital density slightly overestimated in comparison with the $4f_{5/2}(DCH)$ orbital and the density of the PCE corrected $4f_{7/2}(IOTC,IOTC)$ orbital is slightly underestimated at the maximum comparing to the particular DCH orbital, see Fig. 7b. These deviations can be also assigned (as in the case of the p or d orbitals) to the PCE associated with the neglected transformation of the 2-electron (electron-electron) Coulomb terms [38, 49].

The PCE contaminated $4f_{5/2}(IOTC,NR)$ [as well as $4f_{7/2}(IOTC,NR)$] orbital densities are underestimated [overestimated] in the vicinity of the nucleus in comparison with the particular DCH or IOTC orbital densities, see Fig. 7b. On the other hand, at the maximum of the density distribution the PCE contaminated $4f_{5/2}(IOTC,NR)$ and $4f_{7/2}(IOTC,NR)$ orbitals copy the radial distributions of the PCE corrected IOTC $4f_{5/2}$ and $4f_{7/2}$ orbital densities, see Fig. 7c.

For the $4f$ scalar IOTC orbitals, the situation is similar like for the scalar $3d$ IOTC orbital. The IOTC $4f$ orbital can be considered as the SO average of the particular (PCE corrected or contaminated) IOTC $4f_{5/2}$ and $4f_{7/2}$ orbital densities. The PCE in the scalar $4f$ IOTC orbital is significant again only in the vicinity of the nucleus, see Fig. 7b.

Although the DKH2 $4f$ orbitals are not shown in Fig. 7, the conclusions about the IOTC orbitals are completely valid for the DKH2 orbital densities as well (both PCE corrected and contaminated).

4 Conclusions

The total electron density $\rho(IOTC,IOTC)$ closely overlaps with the DCH electron density calculated in the finite basis set approach; independent of the nucleus model, the same agreement is found for the particular s and $p_{1/2}$ orbital densities. The qualitative extent of PCE in the DKH2/IOTC total electron densities is found the same for both the point charge and the finite size nucleus model. The PCE contaminated IOTC/DKH2 orbital densities of the $s(IOTC,NR)$ and $s(DKH2,NR)$ orbitals are grossly overestimated close to nucleus what leads to the large PCE in the total electron densities. In the vicinity of the point charge nucleus, the basis set expansion technique cannot properly cope with

the singular behavior of the numeric $\rho(DCH)$ total electron density, what holds for the s and $p_{1/2}$ orbitals as well.

The PCE corrected (DKH2,DKH2) total electron and $s/2p_{1/2}$ orbital densities are overestimated in the vicinity of nucleus in comparison with the particular DCH or PCE corrected (IOTC,IOTC) densities. The PCE corrected (DKH2,DKH0) densities are even more overestimated in comparison with the particular DCH or (IOTC, IOTC) densities, the (DKH2,DKH1) PCE corrected densities are on the other hand underestimated. Furthermore, the $\rho(DKH2, DKH1)$ contact density and the $\rho_s(DKH2,DKH1)$ contact orbital density are negative if tight enough s type Gaussians are included in the basis set for the point charge model of nucleus. This does not hold for the $p_{1/2}(DKH2,DKH1)$ orbitals, although the global maximum of the radial distribution of the $p_{1/2}(DKH2,DKH1)$ orbitals is not localized at the nucleus. The negative value of the (DKH2,DKH1) electron density is to be regarded as a failure of the DKH1 PCE correction, due to the missing terms of the second order Douglas-Kroll transformation. Although the behavior of the higher order odd PCE corrected DKH electron density at nucleus has not been considered in the presented study, it might be similarly affected as found for the PCE corrected (DKH2,DKH1) total electron and s orbital densities.

Moreover, the PCE corrected scalar DKH2 and IOTC p orbitals have non-zero electron density at nucleus and can be considered as a SO average of the $p_{1/2}$ and $p_{3/2}$ orbitals. The PCE contaminated DKH2/IOTC $p_{1/2}$ and p orbitals have zero electron density at nucleus. The PCE contaminated DKH2/IOTC $p_{3/2}$ orbital densities are overestimated in the region of the maximum of orbital density and in the vicinity of the nucleus comparing to the DCH or PCE corrected DKH2/IOTC $p_{3/2}$ orbital densities.

PCE in the d and f orbital densities is discernable not only in the nuclear region (for the PCE contaminated IOTC/DKH2 densities) but also in the region of the maximum of the radial distribution of orbital densities, where the PCE corrected IOTC/DKH2 orbital densities are deviated from the particular DCH densities due to the PCE associated with the neglected transformation of the 2-electron Coulomb terms.

Furthermore, the PCE corrected (s, p, d) DKH2/IOTC electron densities are nodeless, which is in agreement with the DCH orbital densities (even the scalar PCE corrected orbitals are nodeless), while the PCE contaminated DKH2/IOTC orbitals contain nodes.

Acknowledgments We are grateful to professor K.G. Dyall for his help in regard to the Grasp code, especially for providing to us his version of GRASP code that includes the Gaussian nucleus model. The financial support was obtained from APVV (contract No. APVV-0093-07) and VEGA (contracts No. 1/0817/08 and 1/0127/09). The author DJ would like to thank to ARC and CNRS for funding.

References

1. Pykkö P (1988) *Chem Rev* 88:563
2. Schwerdtfeger P (ed) (2002) Relativistic electronic structure theory, part 1. Fundamental. Elsevier, Amsterdam
3. Dyall KG, Fægri K (2007) Introduction to relativistic quantum chemistry. Oxford University Press, New York
4. Reiher M, Wolf A (2009) Relativistic quantum chemistry. Wiley, Weinheim
5. Iliaš M, Kellö V, Urban M (2010) *Acta Chimica Slovaca* 30:259
6. Dyall KG, Grant IP, Johnson CT, Parpia FA, Plummer EP (1989) *Comput Phys Commun* 55:425
7. Visscher L, Visser O, Aerts PJC, Merenga H, Nieuwpoort WC (1994) *Comput Phys Commun* 81:120
8. Liu W, Hong G, Dai D, Li L, Dolg M (1997) *Theor Chem Acc* 96:75
9. Quiney HM, Skaane H, Grant IP (1999) *Adv Quant Chem* 32:1
10. Abe M, Iikura H, Kamiya M, Nakajima T, Paulovic J, Yanagisawa T, Yanai T, REL4D. homepage: <http://utchem.qcl.t.u-tokyo.ac.jp>
11. Jensen HJAA, Saue TLV with contributions from V. Bakken, Eliav E, Enevoldsen T, Fleig T, Fossgaard O, Helgaker T, Laerdahl J, Larsen CV, Norman P, Olsen J, Pernpointner M, Pedersen JK, Ruud K, Salek P, van Stralen JNP, Thyssen J, Visser O, Winther T (2004) DIRAC04, a relativistic ab initio electronic structure program, Release DIRAC04. <http://dirac.chem.sdu.dk>
12. Jensen HJAA, Saue TLV with new contributions from Bast R, Dubillard S, Dyall KG, Ekström U, Eliav E, Fleig T, Gomes ASP, Helgaker TU, Henriksson J, Iliaš M, Jacob CR, Knecht S, Norman P, Olsen J, Pernpointner M, Ruud K, Salek P, Sikkema J (2008) DIRAC08, a relativistic ab initio electronic structure program, Release DIRAC08. <http://dirac.chem.sdu.dk>
13. van Lenthe E, Baerends EJ, Snijders JG (1993) *J Chem Phys* 99:4597
14. van Lenthe E, Baerends EJ, Snijders JG (1994) *J Chem Phys* 101:9783
15. Hess BA (1985) *Phys Rev A* 32:756
16. Nakajima T, Hirao K (2000) *J Chem Phys* 113:7786
17. Wolf A, Reiher M, Hess BA (2002) Chapter 11. Two-component methods and generalized Douglas-Kroll transformation in relativistic electronic structure theory. Part I. Fundamentals. Elsevier, Amsterdam, p 622
18. Wolf A, Reiher M, Hess BA (2002) *J Chem Phys* 117:9215
19. Wolf A, Reiher M, Hess BA (2004) Recent advances in relativistic molecular theory. World Scientific, Singapore, p 137
20. Barysz M, Sadlej AJ, Snijders JG (1997) *Int J Quant Chem* 65:225
21. Barysz M, Sadlej AJ (2001) *J Mol Struct* 573:181
22. Barysz M, Sadlej AJ (2002) *J Chem Phys* 116:2696
23. Iliaš M, Saue T (2007) *J Chem Phys* 126:064102
24. Kędziera D, Barysz M (2007) *Chem Phys Lett* 446:176
25. Reiher M, Wolf A (2004) *J Chem Phys* 121:2037
26. Reiher M, Wolf A (2004) *J Chem Phys* 121:10945
27. Kutzelnigg W, Liu W (2005) *J Chem Phys* 123:241102
28. Liu W, Peng D (2006) *J Chem Phys* 125:044102
29. Liu W, Kutzelnigg W (2007) *J Chem Phys* 126:114107
30. Sun Q, Liu W, Xiao Y, Cheng L (2009) *J Chem Phys* 131:081101
31. Peng D, Liu W, Xiao Y, Cheng L (2007) *J Chem Phys* 127:104106
32. Liu W (2010) *Mol Phys* 108:1679
33. Wolf A, Reiher M (2006) *J Chem Phys* 124:064102
34. Wolf A, Reiher M (2006) *J Chem Phys* 124:064103
35. Mastalerz R, Lindh R, Reiher M (2008) *Chem Phys Lett* 465:157
36. Barone G, Mastalerz R, Reiher M, Lindh R (2008) *J Phys Chem A* 112:1666
37. Barysz M, Mentel Ł, Leszczyński J (2009) *J Chem Phys* 130:164114
38. Seino J, Uesugi W, Hada M (2010) *J Chem Phys* 132:164108
39. Bučinský L, Biskupič S, Jayatilaka D (2010) *J Chem Phys* 133:1
40. Malkin I, Malkin OL, Malkin VG (2002) *Chem Phys Lett* 361:231
41. Malkin I, Malkin OL, Malkin VG, Kaupp M (2004) *Chem Phys Lett* 396:268
42. Mastalerz R, Widmark PO, Roos BO, Lindh R, Reiher M (2010) *J Chem Phys* 133:144111
43. Knecht S, Fux S, van Meer R, Visscher L, Reiher M, Saue T (2010) *Theor Chem Acc* (accepted)
44. Jayatilaka D, Grimwood DJ (2000) Tonto: a research tool for quantum chemistry. The University of Western Australia, Nedlands, Western Australia, Australia, <http://www.theochem.uwa.edu.au>
45. Saue T, Visscher L and Jensen HJ Aa, with contributions from Bast R, Dyall KG, Ekström U, Eliav E, Enevoldsen T, Fleig T, Gomes ASP, Henriksson J, Iliaš M, Jacob ChR, Knecht S, Nataraj HS, Norman P, Olsen J, Pernpointner M, Ruud K, Schimmelpennig B, Sikkema J, Thorvaldsen A, Thyssen J, Villaume S, Yamamoto S (2010) DIRAC, a relativistic ab initio electronic structure program, Release DIRAC10. <http://dirac.chem.vu.nl>
46. Visscher L, Dyall KG (1997) *Atom Data Nucl Data Tabl* 67:207
47. Dyall KG (2006) *Theor Chem Acc* 115:441
48. Dyall KG Basis sets available at <http://dirac.chem.sdu.dk>
49. Seino J, Hada M (2008) *Chem Phys Lett* 461:327